



HAL
open science

Different in vitro exposure regimens of murine primary macrophages to silver nanoparticles induce different fates of nanoparticles and different toxicological and functional consequences.

Catherine Aude-Garcia, Florent Villiers, Véronique Collin-Faure, Karin Pernet-Gallay, Pierre-Henri Jouneau, Stéphanie Sorieul, Geoffrey Mure, Adèle Gerdil, Nathalie Herlin-Boime, Marie Carrière, et al.

► To cite this version:

Catherine Aude-Garcia, Florent Villiers, Véronique Collin-Faure, Karin Pernet-Gallay, Pierre-Henri Jouneau, et al.. Different in vitro exposure regimens of murine primary macrophages to silver nanoparticles induce different fates of nanoparticles and different toxicological and functional consequences.. *Nanotoxicology*, 2016, 10 (5), pp.586-596. 10.3109/17435390.2015.1104738 . hal-01271894

HAL Id: hal-01271894

<https://hal.science/hal-01271894v1>

Submitted on 29 Apr 2016

HAL is a multi-disciplinary open access archive for the deposit and dissemination of scientific research documents, whether they are published or not. The documents may come from teaching and research institutions in France or abroad, or from public or private research centers.

L'archive ouverte pluridisciplinaire **HAL**, est destinée au dépôt et à la diffusion de documents scientifiques de niveau recherche, publiés ou non, émanant des établissements d'enseignement et de recherche français ou étrangers, des laboratoires publics ou privés.

This article first appeared under the following reference, which should be the only citable form:

Nanotoxicology. 2016 Jun;10(5):586-96. doi: 10.3109/17435390.2015.1104738.

Different in vitro exposure regimens of murine primary macrophages to silver nanoparticles induce different fates of nanoparticles and different toxicological and functional consequences

Catherine Aude-Garcia^{1,2,3}, Florent Villiers^{4,5, 6}, Véronique Collin-Faure^{1,2,3}, Karin Pernet-Gallay^{7,8}, Pierre-Henri Jouneau^{9,10}, Stéphanie Sorieul¹¹, Geoffrey Mure^{1,2,3}, Adèle Gerdil¹², Nathalie Herlin-Boime¹², Marie Carrière^{13,14,*} and Thierry Rabilloud^{1,2,3,*}

¹Univ. Grenoble Alpes, Laboratory of Chemistry and Biology of Metals, Grenoble, F-38000 France.

²CEA Grenoble, iRTSV/CBM, Laboratory of Chemistry and Biology of Metals, Grenoble, F-38054, France.

³CNRS UMR 5249, Laboratory of Chemistry and Biology of Metals, F-38000, Grenoble, France

⁴Univ. Grenoble Alpes, Laboratory of Plant Cellular Physiology, Grenoble, F-38000 France

⁴CEA, iRTSV; Université Grenoble Alpes; CNRS, UMR5168; INRA, USC1359. Laboratoire de Physiologie Cellulaire & Végétale, Grenoble, France

⁵CEA Grenoble, iRTSV/PCV, Laboratory of Plant Cellular Physiology, Grenoble, F-38054, France.

⁶CNRS UMR 5168, Laboratory of Plant Cellular Physiology, F-38000, Grenoble, France

⁷INSERM, U836, F-38042 Grenoble, France

⁸Univ. Grenoble Alpes, Grenoble Institut des Neurosciences, Grenoble, F-38042, France

⁹Univ. Grenoble Alpes, INAC-SP2M, F-38000 Grenoble, France.

¹⁰CEA, INAC-SP2M, F-38054 Grenoble, France.

¹¹CNRS, IN2P3, CENBG, UMR5797, F-33175 GradignanCedex, France.

¹²URA2453 CEA-CNRS, NIMBE, LEDNA, Laboratoire Francis Perrin (LFP), CEA Saclay, F-91191 Gif sur Yvette, France.

¹³Univ. Grenoble Alpes, INAC-SCIB, F-38000 Grenoble, France.

¹⁴CEA, INAC-SCIB, F-38054 Grenoble, France.

*Corresponding authors: Thierry Rabilloud, CEA Grenoble, ProMD, Bât C3, 38054 Grenoble Cedex 9, France. Phone: +33 4 38 78 32 12. thierry.rabilloud@cnrs.fr. Marie Carrière, CEA Grenoble, LAN, Bât C5, pce 632, 38054 Grenoble Cedex 9, France. Phone: +33 4 38 78 03 28, fax: +33 4 38 78 50 90. marie.carriere@cea.fr; these authors contributed equally to this work.

Abstract

Silver nanoparticles (Ag-NPs) are used in a variety of consumers' goods. Their toxicological impact is currently intensely studied, mostly upon acute exposure, but their intracellular dissolution and fate is rather poorly documented.

In this study murine primary macrophages were exposed to a single high but non-lethal dose of Ag-NPs or to repeated, low doses of Ag-NPs. Cells were either collected immediately after acute exposure or after 72 h of recovery in NP-free exposure medium. Ag intracellular content and distribution were analyzed by particle-induced X-ray emission (PIXE), transmission electron microscopy coupled to energy-dispersive spectroscopy analysis (TEM-EDS) and inductively-coupled plasma mass spectrometry (ICP-MS). In parallel, macrophage functionality as well as inflammatory and thiol-responses were assessed after Ag-NP exposure.

We show that Ag accumulation in macrophages is similar upon acute and repeated exposure to Ag-NPs, and that Ag is partly expelled from cells during the 72 h recovery stage. However, acute exposure leads to a strong response of macrophages, characterized by reduced mitochondrial membrane potential, phagocytic capacity and NO production upon LPS stimulation. Under this condition, we also show an increased release of pro-inflammatory cytokines as well as a decreased release of anti-inflammatory cytokines. This response is reversible since these biomarkers reach their basal level after the recovery phase; and is much less intense in repeatedly-exposed cells.

These results suggest that repeated exposure of macrophages to Ag-NPs, which is a more realistic exposure scenario than acute exposure, leads to significant Ag intracellular accumulation but a much less intense toxicological response.

Keywords nanoparticle, silver, macrophage, speciation, toxicity

Introduction

Silver nanoparticles are currently used in a broad spectrum of commercial products, including consumers' goods and medical products. This extensive use as well as the known ecotoxicity of silver ions (Ratte, 1999) makes Ag-NPs one of the most studied nanoparticles in terms of toxicological and ecotoxicological impact. The major source of Ag-NP toxicity has been attributed to the release of Ag⁺ ions, particularly in bacterial models, although there may also be a nano-specific effect (Fabrega, 2009; Sotiriou, 2010; Xiu, 2011; Xiu, 2012). Toxicity studies have been conducted on bacterial models, *in vitro* eukaryotic cells, and on *in vivo* animal models. Results from these studies as well as possible mechanisms of Ag-NP toxicity have been largely reported (Chernousova, 2013; Dos Santos, 2014). Still, the fate and chemistry of Ag-NPs have rarely been studied in the cellular context, and has not been correlated with relevant toxicological endpoints upon realistic exposure scenarios such as repeated exposure (mimicking exposure of the population to daily life products) or acute exposure followed by a recovery stage (mimicking accidental exposure).

As a Pearson's soft Lewis acid, Ag(I) tends to complex with soft Lewis bases; it therefore exhibits a strong affinity for sulfur. Consequently, in biological and environmental samples the major species that may complex Ag(I) are organosulfur compounds, i.e. compounds containing sulfur such as glutathione, cysteine or proteins such as metallothioneins, sulfides or compounds containing polysulfides with at least one free S⁻ (Bell, 1999). In the environment, Ag-NP transformation is governed by surface sulfidation, which forms Ag₂S (Elechiguerra, 2005; Kaegi, 2011; Kim, 2010; Levard, 2011; Liu, 2011; Reinsch, 2012). In mammalian cells, Ag-NPs accumulate via endocytosis as do most NPs (Oh, 2014). Upon reaching the endosomal/lysosomal compartment, Ag⁰ from Ag-NPs oxidizes to Ag(I) leading to NP dissolution and recombination with either chloride ions or thiols from intracellular organosulfur compounds. The most potent intracellular sulfur-containing ligands that might form complexes with Ag⁺ ions are metallothioneins, glutathione (GSH) and cysteine, since their concentration in mammalian

cell cytoplasm is high, e.g. 0.1 to 1 mmol/L for GSH (Meister, 1988) and their stability constant with Ag ions is high ($K \sim 10^{13}$) (Bell, 1999). Ag-NP toxicity depends on the rate of dissolution of NPs in the lysosomal compartment, itself depending on the surface charge of Ag-NP (Setyawati, 2014). Recently, Ag(I) recombination with intracellular thiols has been demonstrated by us and others, either in mouse primary macrophages chronically or acutely exposed to Ag-NPs coated with PVP (Veronesi, 2015), in THP-1 monocytes acutely exposed to Ag-NPs coated with Tween 20 (Wang, 2015) or CHO-K1 hamster ovary cells acutely exposed to Ag-NPs synthesized chemically by reduction of silver nitrate (Jiang, 2014). NPs are taken up by cells via both lipid-raft-mediated endocytosis and passive diffusion through the plasma membrane, and rapidly dissolve in the intracellular compartment (Jiang, 2014). X-ray absorption spectroscopic (XAS) analysis proves that, in two of these studies, Ag-NPs are first oxidized and then recombine with intracellular sulfur-containing ligands (Jiang, 2014; Wang, 2015) rather identified as being metallothioneins (Wang, 2015). This accumulation and/or dissolution of NPs causes reactive oxygen species production in cells as well as cytotoxicity (Jiang, 2014; Wang, 2015) and apoptosis (Wang, 2015). By also using XAS, we reported that Ag-NPs coated with PVP dissolve in mouse primary macrophages exposed to Ag-NPs either in acute mode (24 h, 5 $\mu\text{g}/\text{mL}$) or in repeated mode (4 days, 1.25 $\mu\text{g}/\text{mL}$ per day). Then Ag ions coordinate with intracellular thiols with a coordination chemistry and bond length compatible with digonal Ag_2S sites, i.e. GSH is the most likely putative ligand (Veronesi, 2015). We did not detect any intermediate coordination chemistry where Ag is combined with O. GSH is an essential element of the oxidative stress response, and oxidative stress is one of the major mechanisms underlying NP cytotoxicity. Ag ion recombination with GSH may thus be detrimental to macrophage survival and function. For this reason, in the present article we explored the biological consequences of this Ag-NP dissolution and recombination with GSH.

Macrophages are the main scavenger cells in the body, and as such they are in charge of removing exogenous material from the bloodstream and organs by phagocytosis, particularly

NPs. They are also in charge of removing bacteria from the body. Therefore it is all the more important to clearly understand the interaction between macrophages, bacteria and the Ag-NPs which are often used as bactericidal agents (Yilma, 2013). Moreover, macrophages are a key cell type in the immune response and in inflammation leading sometimes to pathological developments such as in asbestosis and silicosis (Hamilton, 1980). As a consequence, the modulation of their functions following exposure to NPs is also worth studying (Nishanth, 2011; Xu, 2013). Despite the fact that the interaction of Ag-NPs with macrophages has been studied at various levels in acute exposure conditions (Pratsinis, 2013; Singh, 2012) little is known about how macrophages cope with Ag-NPs either after repeated exposure to a non-toxic dose or after a post-exposure recovery period. Moreover no direct correlations between the real state of NPs within the cell and the alteration of macrophage functions have been reported.

The present study aimed at going beyond the state of the art and investigating the fate and toxicological impact of Ag-NPs on a relevant cell model and in more realistic exposure scenarios. To achieve this goal, we focused on post-mitotic primary murine macrophages, which contrary to cell lines do not divide but still preserve their metabolic activity. They are consequently more physiologically relevant than dividing macrophage cell lines. These macrophages were exposed to sub-lethal concentrations of Ag-NPs either in acute mode (24 h, 5 $\mu\text{g}/\text{mL}$) or in repeated mode (4 days, 1.25 $\mu\text{g}/\text{mL}$ per day) or in acute mode followed by a recovery period (24 h, 5 $\mu\text{g}/\text{mL}$ then 72 h of recovery in cell culture medium) as in our previous study where we showed that Ag-NPs dissolved and Ag ions recombined with sulfur-containing ligands that were probably GSH (Veronesi, 2015).

Material and methods

Nanoparticle physico-chemical characterization

Spherical Ag-NPs (<100nm) coated with PVP40 were purchased from Sigma-Aldrich (catalog number 758329) as a 5 wt. % dispersion in ethylene glycol. Working NP suspensions were prepared by dilution in deionized water. The hydrodynamic diameter and the particle size distribution were characterized by dynamic light scattering (DLS) after dilution in water and in complete culture medium using a Wyatt DynaproNanostar instrument.

Cell culture and exposure

Bone marrow-derived macrophages were obtained from 6- to 8-week-old C57BL/6 mice and differentiated during 10 days as described previously (Schleicher, 2009; Triboulet, 2013). They were cultured at 37°C in a humidified 5% CO₂ incubator for no more than 2 weeks. For exposure to NPs, several schemes were used. In the acute exposure condition, macrophages were exposed to 5 µg/ml Ag-NPs for 24 hours in complete medium (i.e. cell culture medium containing serum). Cells were then harvested immediately after this exposure period (Sc1A). In the recovery condition (Sc1R), the cells were exposed for 24 hours to 5 µg/ml Ag-NPs, then the medium was removed, the cells were rinsed once with complete medium, and cultured again for 72 hours in complete medium without nanoparticles and with no further medium change. In the repeated exposure condition (Sc2), 1.25 µg/ml Ag-NPs were added to the macrophages every day for four days. Cells were harvested at the end of the four days exposure period. Two control conditions were tested, a control without silver, and a control with silver lactate, in which macrophages were exposed for 24 hours to 5 µM, i.e. 0.985 µg/ml silver lactate in complete medium, corresponding to 0.535 µg/mL of silver ion. This dose of silver ion leads to the same cytotoxicity as 5 µg/ml Ag-NPs.

Silver assay by ICP-MS

For measuring the Ag-NP dissolution, NPs were added at 5µg/ml in 5 mL of complete culture medium (i.e. containing 10% fetal calf serum) in 25cm² culture flasks for 24 or 96 h. After this time the medium was recovered, an aliquot was saved, and the remaining was centrifuged at 400,000g for 30 minutes to pellet the nanoparticles. The supernatant was saved and the pellet resuspended in 1 ml of buffer A (Hepes 50 mM pH 7.5, sorbitol 200mM, magnesium acetate 2mM). The saved aliquot, the supernatant and the resuspended pellet were mineralized by the addition of one volume of suprapure HNO₃ 65% and incubation on a rotating wheel at room temperature for 18 h.

After dilution in 1%[v/v] suprapure HNO₃ 65%, 107 and 109 m/z were quantified on an inductively coupled plasma mass spectrometer (ICP-MS, Hewlett-Packard 4500 Series, Agilent Technologies, Massy, France) equipped with a Babington nebulizer and a Peltier-cooled double-pass Scott spray chamber. Three biological replicates were assayed, each 3 times from independent dilutions of the original mineralized sample. Analysis parameters were set to 1s integration time, 3 repetitions, detection of m/z - 0.05, m/z and m/z + 0.05. Total element content was determined against a standard curve made of a serial dilution of silver lactate in complete culture medium.

For determining the fate of nanoparticles, the same experiment was carried out on flasks containing cells. After incubation under the different regimens described above, the conditioned culture medium was saved and the cells were scraped in 5 ml of buffer A. The cells were then lysed by the addition of hexadecyltrimethylammonium acetate (2% w/v final concentration) and incubation on a rotating wheel at room temperature for one hour. The conditioned media and cell lysates were then ultracentrifuged (400,000g; 30 minutes) and the respective supernatants and pellets processed as described above.

Particle-induced X-ray emission

Micro-particle-induced X-ray emission (PIXE) and Rutherford Backscattering (RBS) analyses were carried out on cells seeded on thin polycarbonate foils and exposed to Ag-NPs. Membranes were rinsed twice with PBS, cryofixed by immersion in isopentane chilled to $-160\text{ }^{\circ}\text{C}$ in liquid nitrogen (Carriere, 2005). Samples were freeze-dried for 24 h at $-10\text{ }^{\circ}\text{C}$, 0.37 mbar. Micro-PIXE and micro-RBS spectra were recorded simultaneously on the beamline of the AIFIRA platform (CENBG, Bordeaux, France) (Barberet, 2009). The 3.5 MV Singletron accelerator (HVEE) was adjusted in order to deliver a focused beam ($2.5\text{ }\mu\text{m}$) of 3 MeV protons, with a beam current of 1 nA. X-rays were detected with a $80\text{ mm}^2\text{Si(Li)}$ detector (Gresham, energy resolution: 160 keV) orientated at 135° with respect to the incident beam axis, and equipped with a $12\text{ }\mu\text{m}$ thick beryllium window. A funny filter (Al, thickness $200\text{ }\mu\text{m}$, % hole = 1 mm) was used in order to limit the dead-time (Rate $\sim 500\text{ cps/s}$, dead time below 10%). Backscattered protons were recorded at 135° with a silicon PIPS detector (Canberra, 50 mm^2 , thickness $100\text{ }\mu\text{m}$, resolution: 17 keV). Four elemental maps of $100\times 100\text{ }\mu\text{m}^2$ were recorded on each sample, and drawn using the Supavisio software (<http://biopixe.free.fr>). For Ag intracellular content measurement, data were fitted using SIMNRA (RBS) (Mayer, 2002) and Gupix (X-ray spectra) (Maxwell, 1995) as described previously (Brun, 2014) and normalized thanks to analysis of KI, NaCl and ZnTe standards (Carmona, 2008), kindly provided by Dr. R. Ortega.

Electron microscopy

After exposure, cells were fixed with 2.5% glutaraldehyde, post-fixed with OsO_4 and dehydrated in graded concentrations of ethanol then embedded in Epon, as described elsewhere (Brun, 2014). Ultra-thin sections were cut (80 nm), counterstained with uranyl acetate and observed with a JEOL 1200 EX transmission electron microscope (TEM) operated at 80 kV (Grenoble Institut des Neurosciences, France). They were also observed using a FEI/Tecnai Osiris

scanning/transmission electron microscope (STEM), operated at 80 kV; then electron-dense deposits were analyzed by energy-dispersive spectroscopy (EDS) on the same equipment.

Phagocytosis Activity measurement

The phagocytic activity was measured using fluorescent latex beads (1 μm diameter, green-labeled, catalog number L4655 from Sigma-Aldrich). The beads were pre-incubated at a final concentration of 55 mg/ml for 30 min at 37 °C in a 1:1 (v/v) PBS/FCS solution. Cells were first exposed to Ag-NPs following either scenario 1A or 1R or 2, then to fluorescent latex beads (5.5 mg/l final concentration) for 3 h. The cells were then harvested, washed with cold PBS. In order to remove beads adhering to the cell surface, 3 ml of water and 1 ml of 3.5% NaCl were added on each cell pellet. After another wash with cold PBS the resulting fluorescence of the cells was measured by flow cytometry on a FACS Calibur cytometer equipped with CellQuest software (Becton Dickinson) as described previously (Abel, 1991; Triboulet, 2013).

Mitochondrial transmembrane potential

The mitochondrial transmembrane potential was estimated with a test based on Rhodamine 123 uptake (Johnson, 1980) as described previously (Triboulet, 2013). Briefly: cells were first exposed to Ag-NPs following either scenario 1A or 1R or 2. At the end of the exposure time, they were incubated with 10 $\mu\text{g/ml}$ Rhodamine 123 for 30 min at 37°C, harvested, rinsed twice in cold PBS and analyzed by flow cytometry on a FACS Calibur cytometer (Becton Dickinson) using fluorescein excitation/emission filters.

Measurement of intracellular reduced glutathione

Intracellular glutathione levels were measured using monochlorobimane (mCB), a thiol-reactive cell permeable reagent that binds to intracellular reduced glutathione (GSH) forming a fluorescent adduct (Hedley, 1994). After treatment of cells with Ag-NPs or Ag lactate under the

exposure regimen described above, mCB was added to the macrophages and incubated for 5 min at 37°C, then the cells were incubated on ice for another 5 min as described previously (Aude-Garcia, 2011). They were washed with PBS then the cellular fluorescence was analyzed by flow cytometry under UV excitation using a Moflo cytometer (Dako).

NO production

Macrophages were exposed to Ag-NPs according to the different scenarios then we added 5 mM Arginine monohydrochloride to the cells, which gives a high concentration of substrate for the nitric oxide synthases. Finally, 1 µg/ml of LPS was added to half of the cells. After 18h of incubation, the cell culture medium was sampled and centrifuged at 10,000 *xg* for 10 min to remove cells and debris. We then added an equal volume of Griess reagent in it and after incubation for 30 min at room temperature, absorbance at 540 nm was read and the nitrite concentration was determined using a standard curve prepared in the same conditions.

Cytokine Assays

TNF- α , IL-6 and IL-10 concentrations in the culture supernatants were measured using the Cytometric Bead Array (CBA) mouse inflammation kit (BD Pharmingen) according to the manufacturer's instructions. The measures were performed on a FACSCalibur flow cytometer and the data were analyzed using CellQuest software (Becton Dickinson).

Statistical analysis

Data are expressed as mean \pm standard deviation. Statistical tests were run using Statistica 7.1 software (Statsoft, Chicago, IL, USA). As normality assumptions for valid parametric analyses were not satisfied (Kolmogorov-Smirnov tests), non-parametric one-way analyses of variance on ranks approach (Kruskal-Wallis) were used. When significance was demonstrated ($p < 0.05$), paired comparisons were run using either Mann-Whitney U-test or Student's T-test.

Results

NP physico-chemical characterization

In the present study we used commercial silver nanoparticles, coated with PVP and suspended in ethylene glycol. These NPs were characterized in our laboratory prior to any biological experiment. They were spherical and their average diameter was 59 ± 18 nm, with grain size ranging from 25 to 100 nm as measured by transmission electron microscopy (Figure S1A-C). Upon dilution in cell culture medium their hydrodynamic diameter reached 95.7 nm, as measured by DLS (Figure S1D). Their zeta potential was -22.1 mV. They were stable, i.e. we did not observe any aggregation and/or agglomeration for at least 4 days (Table S1).

Intracellular accumulation, distribution and cytotoxicity

Murine primary macrophages were exposed to a single, high dose of Ag-NPs (5 $\mu\text{g}/\text{mL}$, 24 h, Sc1) or to repeated, low doses of Ag-NPs (1.25 $\mu\text{g}/\text{mL}$ per day, 96 h, Sc2). Cells exposed in scenario 1 were then collected immediately after exposure (Sc1A) or after 3 days of recovery in NP-free exposure medium (Sc1R).

Cytotoxicity was evaluated by using the trypan blue exclusion assay; none of these scenarios induced overt cell mortality (see Figure S2 for mortality rate in Sc1A).

Ag intracellular content was measured by using particle-induced X-ray emission (PIXE) (Figure 1). Intracellular accumulation was significant in cells exposed at 5 $\mu\text{g}/\text{mL}$ for 24 h (Sc1A) and at 1.25 $\mu\text{g}/\text{mL}$ per day for 96 h (Sc2). It reached 10.6 ± 3.2 $\mu\text{g}/\text{cm}^2$ and 17.5 ± 3.6 $\mu\text{g}/\text{cm}^2$, respectively, these amounts being not significantly different from one another. In these conditions, our previously published results show that in Sc1A 61.1% of the Ag content is still present as Ag-NPs and 38.9% is recombined with GSH, while in Sc2 27.3% of the Ag content is

present as Ag-NP and 73.7% is recombined with GSH (Veronesi, 2015). Conversely, in cells exposed to Ag-NPs for 24 h and then allowed to recover for 72 h (Sc1R) Ag content was significantly lower, with $5.6 \pm 0.6 \mu\text{g}/\text{cm}^2$. Ag content in cells exposed to Ag-lactate was not significantly different from Ag content in unexposed cells.

Transmission electron microscopy (TEM) observations showed no major alterations of macrophage morphology in these exposure scenarios. Electron-dense structures were clearly visible in Ag-NP-exposed cells but not in unexposed cells (Figure 2A-B); they were trapped in cytoplasmic vesicles that look like late endosomes or autophagosomes, as classically described with NPs (Oh, 2014). These electron-dense structures showed various morphologies. At 24 h post-exposure (Sc1A), they looked like loose agglomerates of NPs (Figure 2C-D, arrows) combined to layered structures (Figure 2C-D, crosses). Both structures were also observed in cells exposed for 24 h after 72 h of recovery (Sc1R, Figure 2E-F, arrow and crosses). Conversely after repeated exposure at low concentration (Sc2), we still observed loose agglomerates of NPs (Figure 2G-H, arrows) but also some very dense, condensed spherical structures (Figure 2G-H, §). In this condition we never observed the layered structures. The chemical composition of these structures was identified by energy-dispersive spectroscopy (EDS) (Figure 2I-L). All of them contained Ag which was clearly correlated with the presence of sulfur (S), confirming that Ag-ions were recombined with sulfur-containing ligands and showing that this recombination led to Ag precipitation. They also contained Os, resulting from the fixation and staining procedure of TEM grid preparations, and Si and Al contaminations that were also observed in non-electron-dense areas. No electron-dense deposits were observed in cells exposed to Ag-lactate (data not shown).

To complement these data, we measured the Ag-NP dissolution/re-precipitation and accumulation in cells and in the media by ICP-MS (Table 1). These experiments showed that nanoparticles dissolution was low even in complete culture medium, and that this extracellular dissolution could not account for the observed nanoparticles toxicity. Interestingly, the addition of

silver ions in the complete culture medium resulted in a partial precipitation of the silver in a physical form that sedimented upon centrifugation. These experiments also provided an estimation of the uptake of nanoparticles by the cells, and confirmed the fact that the cells could excrete silver during the recovery period. The conditioned medium in which the cells recovered contained a smaller soluble fraction of silver than the NP-supplemented medium used for cell treatment.

Finally, silver quantification showed a constant soluble amount within the cells, irrespective of the initial treatment. When a ten-fold lower amount was used for treatment (ionic silver), it resulted in a ten-fold higher percentage of soluble silver recovered in the cells.

Induction of a thiol response

As heavy metal ions (and surfaces) are thiophilic, they bind to thiols from cells which can be either low molecular weight sulfur-containing ligands such as GSH, which depletion induces oxidative stress, or cysteine groups from proteins. Binding to cysteine-containing proteins often leads to their inactivation; this is for example one of the major determinants of zinc toxicity (Dineley, 2003). To counteract this toxic effect, cells induce metallothioneins (MTs) which are dedicated metal-scavenging proteins. They can also increase their glutathione production. We tested both of these endpoints by measuring the intracellular GSH levels (Figure 3) and the mRNA expression of MT-I and MT-II (Figure S3) in macrophages exposed to Ag-NPs.

The concentration of free GSH decreased after acute exposure to Ag-NPs (Figure 3, sc1A), providing additional proof of the complexation of Ag with GSH that we previously demonstrated by X-ray absorption spectroscopy (Veronesi, 2015). However, cells restored their basal GSH levels during recovery and a slightly higher GSH content was even observed in this condition (Figure 3, sc1r) suggesting that Ag stress is not acute enough to induce depletion of GSH. Conversely after repeated exposure to low concentrations of Ag-NPs, the intracellular GSH level was not significantly reduced (Figure 3, sc2).

Macrophages massively induced MT-I and MT-II (Figure S3) in response to Ag-NPs, in all exposure modes. The induction rate reached 55-fold and 310-fold for MT-I and MT-II, respectively, in acutely-exposed cells. Although always very high, the extent of induction correlated with the instantaneous concentration of Ag, as shown by higher induction of MTs in Sc1, as compared to Sc2.

Effect of silver nanoparticles on macrophage functions

When investigating the effects of these silver nanoparticles on macrophage functions, part of the effects observed could be attributable to the PVP coating of the nanoparticles. However, we know from previous work (Triboulet, 2015) that PVP has no intrinsic effects, so that the observed effects are due to the silver itself.

A frequent mechanism involved in metals toxicity is the perturbation of normal mitochondrial function. For zinc such perturbation has been shown to occur via the inhibition of several mitochondrial matrix enzymes (Gazaryan, 2007; Lemire, 2008), and for copper via a perturbation of the respiratory complexes (Triboulet, 2013). We therefore measured the mitochondrial transmembrane potential as a crude and global indicator of the mitochondrial function (Figure 4A). The results show that acute exposure to Ag-NPs induced an important decrease in the mitochondrial transmembrane potential, which is partly reverted during the recovery period. This decrease was also significant, although less intense, upon repeated exposure to Ag-NPs (Sc2).

Beside this general cellular function, we also examined specialized macrophage functions, namely the phagocytic capacity and the LPS-induced NO production. Our results show that acute exposure to Ag-NPs induced a strong decrease of both macrophage functions, which was partially reverted during the recovery process (Figure 4B-C). Interestingly, the mode of exposure also played a key role. At equal final Ag intracellular contents, repeatedly-exposed cells were much less altered than acutely-exposed cells, following the general "health pattern" already

described in the other endpoints. Within this general frame, the only discordant point was the trend, although it was not statistically significant ($p=0.052$) of NO synthesis reduction in cells exposed to Ag-lactate. This may however just represent an extension of the well-known repression of NO production by macrophages in the presence of heavy metal ions (Tian, 1996). Finally we tested the capacity of Ag-NP-exposed macrophages to secrete cytokines upon LPS induction. Our results showed that acute exposure led to an increased release of pro-inflammatory $\text{TNF}\alpha$ and IL-6 cytokines (Figure 5A-B), whereas they caused a decreased release of IL-10, an anti-inflammatory cytokine (Figure 5C). Again, after a period of recovery, these effects were reverted, and the secretion of cytokines nearly reached their basal level. These effects were much less intense in macrophages repeatedly exposed to Ag-NPs (Figure 5A-C).

For better clarity, we summarized all these results in Table 2.

Discussion

The vast majority of *in vitro* toxicological work on Ag-NPs has been carried out on cell lines acutely exposed to high concentrations of NPs. These experiments are crucial to identify which cellular mechanisms are altered by Ag-NPs and how NPs exert their toxic effects. However, this rather short time frame only allows for the investigation of the initial phases of NP interaction with cells, i.e. their internalization and their intracellular or extracellular dissolution. This has led to the concept of the Trojan horse effect (Park, 2010) and to showing that the toxicological contribution of dissolved Ag ion varies with respect to the size of NPs (Pratsinis, 2013). This is also why we used only a large-sized, PVP-coated nanoparticle, in order to avoid confounding effects linked to silver ion release (Beer, 2012; Pratsinis, 2013) which occurs even upon storage for smaller nanoparticles (Kittler, 2010). However, these studies must be accompanied by *in vitro* studies on a longer time frame for several reasons. First of all, as heavy metals are considered as

persistent toxicants, it is important to assess the persistence of Ag in cells after acute exposure, as well as the (ir)reversibility of the cellular effects they induce. Second, in daily-life products Ag-NPs are often used in slow delivery forms, e.g. in plasters. It is then necessary to investigate how cells cope with such a slow delivery, both at the level of NP handling and at the functional level. In addition to their physiological relevance, the use of post-mitotic primary macrophages is particularly relevant for such studies, as it prevents any interferences and signal dilutions coming from dividing cells such as cell lines. It also avoids any abnormalities present in cell lines due to the immortalization/transformation process. The only issue is that the lifespan of *in vitro* primary mouse macrophages is limited to one week post-terminal differentiation. Consequently it does not allow for real long-term chronic exposures, mimicking occupational exposure or exposure via ingestion of contaminated food. This is why we used shorter term, repeated exposures. Nevertheless, our results clearly show that cells handle Ag-NPs in a more complex way than anticipated, and that the response differs at high and low dose.

The effects of acute exposure are reversible

First of all, when cells are allowed to recover in a NP-free medium after acute exposure to Ag-NPs, they do eliminate Ag rather rapidly, as shown by our PIXE experiments. This is in sharp contrast with the very slow elimination of gold nanoparticles that has been described in Kupffer cells (Sadauskas, 2009) but confirms what was previously shown by Wang et al. on THP-1 monocytes exposed to Ag nanoparticles (Wang, 2015). Moreover the intracellular electron-dense structures containing Ag that we observe in TEM show the same shape directly after acute exposure and after the recovery period. Our experiments suggest that the efflux of silver is mainly in a sedimentable form, and may correspond to exocytosis of the nanoparticles and/or to the excretion of linear, high molecular weight silver-GSH complexes that forms in cells upon exposure to these Ag-NPs, as recently described (Veronesi, 2015). Decrease of intracellular

Agcontent explains in turn how cells recover their functions to a large extent, as we observed from the measurement of mitochondrial membrane potential, phagocytosis activity, NO production and cytokine release upon LPS stimulation. It also explains the modulation of intracellular GSH content, which drops after acute exposure, and then is higher after the recovery period than in unexposed cells. The drop after acute exposure suggests that GSH is used by the cells to chelate potentially toxic Ag ions, as also suggested in our previously published study (Veronesi, 2015). Induction after the recovery phase suggests that cells respond to acute Ag stress by inducing *de novo* production of GSH in order to reestablish redox balance. Still, even if all these effects are reversible, it is important to note that acute exposure to Ag-NP deeply affects macrophage functions, which is in agreement with previous studies (Chernousova, 2013; Dos Santos, 2014).

Acute vs. repeated exposure

When cells are exposed to the same dose of Ag-NPs but provided either as a single dose or as a four-split dose, the amount of internalized Ag is similar, as shown by our PIXE and ICP-MS experiments. The speciation of intracellular Ag is the same upon both exposure schemes, i.e. Ag combined with sulfur-containing ligands, and we show that the proportion of Ag combined to -S is much higher in cells exposed repeatedly to Ag-NPs than it is in acutely exposed cells (Veronesi, 2015). Moreover, we observe a more intense response in cells exposed in acute mode. Indeed in acutely-exposed cells mitochondrial membrane potential, phagocytic capacity, NO and IL-10 productions upon LPS stimulation are drastically reduced whereas productions of TNF α and IL-6 are increased. Conversely all these functions are only poorly affected in repeatedly-exposed cells. One hypothesis is that, in the repeated exposure scheme, cells have enough time and resources to produce a response against Ag stress. Cells may progressively passivate the surface of Ag-NPs, rendering it less reactive, by direct transition from an Ag⁰ surface to an Ag-S surface. Such a process is likely to inhibit the release of Ag ion from NPs,

which is recognized as being at the origin of Ag-NP toxicity(Levard, 2012; Levard, 2011; Mulley, 2014; Reinsch, 2012). Additionally it might explain the condensed, rather spherical shapes of Ag-containing deposits that we observe by TEM in repeatedly-exposed cells, which can be interpreted as Ag-NPs covered by their passivated shell, as previously observed in environmental conditions(Levard, 2011).Still, we have no direct evidences of surface passivation; another explanation would be the release of Ag ions from Ag-NPs, then recombination with thiols (e.g. glutathione) as spheroidal, condensed deposits.

Conversely, in cells exposed to Ag-NPs in acute mode, NPs may rapidly release high amountsof Ag ions, to which cells respond immediately by chelation with all the sulfur-containing molecules that are available, i.e. principally glutathione and sulfur-containing proteins (Babula, 2012; Meister, 1988). It has recently been suggested that the low pH in lysosomes had only a minor role in NP dissolution (Jiang, 2014) suggesting that the presence of sulfur-containing ligands itself caused extraction of Ag ions from the surface of NPs. Our TEM observations show that this extraction and recombination with sulfur-containing ligands, either glutathione or cysteine-containing proteins, results in precipitated layered structures dispersed throughout the cytoplasmic compartment in which Ag-NPs are accumulated.When the available glutathione resource is saturated, Ag-NPs still release some Ag ions that may exert toxic effects in cells. Ag ion-induced toxicity has been reported to result from reactive oxygen species(ROS) production triggered by NPs themselves, or because the release of Ag ions may deprive cells from crucial actors of redox balance reestablishment, such as GSH(Kim, 2011; Navarro, 2008). Some reports suggest that Ag-NP toxicity results from both ROS dependent and ROS-independent pathways (Chairuangkitti, 2012; Jiang, 2014).Since the decrease of mitochondrial membrane potential, phagocytic capacity and NO production upon LPS stimulation can all be caused by oxidative stress our results rather support the hypothesis of oxidative stress-induced Ag-NPs toxicity.We also show that cells react to this influx of Ag ions by inducing a thiol-response, and consequently reestablishing their basal intracellular glutathione and metallothionein levels.

Induction of metallothionein mRNA expression is observed upon both acute and repeated exposure, and it is a long-term response since it is also observed after the recovery period. Interestingly, the amount of soluble silver in cells is almost constant under all conditions, and may correspond to the upper tolerable limit for cells.

In summary, our results suggest that acute response of cells to Ag-NPs is rather dissolution and re-precipitation of Ag ions with soluble and directly available SH-containing ligands, forming layered structures composed of Ag and S. Conversely the long-term response to low concentrations of Ag-NPs may also cause precipitation of Ag ions with SH-containing ligands, but rather as condensed spherical structures. This corresponds to the two mechanisms of oxysulfidation reported by Liu et al. in environmental conditions (Liu, 2011). This result underlines the preeminent role of kinetics in the cellular mechanism of Ag-NPs handling by cells, as well as in their toxicity.

When using the results gathered across our series of experiments, a simple model can be proposed:

In the case of an acute exposure to a high but non-lethal dose, there is a massive release of silver ion that binds to all intracellular thiols, including GSH, which severely compromises the energetics of the cells, as shown by the mitochondrial dysfunction. Nevertheless the cells are able to mount a response, as shown by the massive induction of metallothioneins. In a subsequent stage, metallothioneins scavenge the free silver ions and store them before they are progressively eliminated during recovery. In the case of a repeated exposure, the initial dose is low enough not to disturb the cellular functions too severely. The cells react by increasing the production of their sulfur-containing scavengers, such as GSH and metallothioneins, so that incoming nanoparticles are immediately scavenged by thiols. This mechanism explains how, upon repeated exposure, cells can internalize the same amount of silver than in the case of an acute exposure and still be largely functional.

Conclusions

Upon more realistic exposure scenarios, i.e. repeated exposure to low concentrations of Ag-NPs or acute exposure to Ag-NPs followed by a recovery phase, our results show that primary murine macrophages i) accumulate high amounts of Ag, ii) recombine intracellularly-dissolved Ag ions with SH-containing ligands, and iii) eventually release some Ag from cells. In these conditions their functionality is much less affected than upon acute exposure scenarios. These conclusions are of high importance in a risk assessment perspective; they show that the cellular response to acute *in vitro* exposure, i.e. exposure to high concentrations of NPs for short times, does not necessarily reflect the cellular response to exposure to NPs in environmentally-realistic conditions.

Acknowledgements

This work was funded by ANSES (PNREST 2011/25, Innimmunotox project) and by the CEA toxicology program (Nanostress grant). It is a contribution to the Labex Serenade (n° ANR-11-LABX-0064) funded by the « Investissements d'Avenir » French Government program of the French National Research Agency (ANR) through the A*MIDEX project (n° ANR-11-IDEX-0001-02). STEM-EDS analyses were obtained with the TEM OSIRIS, Plateform Nano-Safety, CEA-Grenoble, operated by P.H. Jouneau. This work was supported by France and managed by Agence National de la Recherche (ANR), program 'Investissements d'Avenir', reference ANR-10-EQPX-39.

Author contributions

C. Aude-Garcia carried out primary macrophage preparation and Ag-NP exposure, as well as the whole biological assessment, with the help of G. Mure and T. Rabilloud. F. Villiers carried out ICP-MS analyses. V. Collin-Faure was involved in the FACS analyses. K. Pernet-Gallay, M.

Carrière and PH Jouneau performed TEM, STEM and EDS observations and analyses. S. Sorieul and M. Carrière recorded and analyzed PIXE data. A. Gerdil and N. Herlin-Boime carried out NP physico-chemical analysis. C. Aude-Garcia, M. Carrière and T. Rabilloud conceived the study and wrote the manuscript. All the authors read and approved the manuscript.

Declaration of interest

The authors declare that there are none.

References

- Abel G, Szollosi J, Facht J. 1991. Phagocytosis of fluorescent latex microbeads by peritoneal macrophages in different strains of mice: a flow cytometric study. *Eur J Immunogenet* 18(4): 239-45.
- Aude-Garcia C, Villiers C, Candeias SM, Garrel C, Bertrand C, Collin V, Marche PN, Jouvin-Marche E. 2011. Enhanced susceptibility of T lymphocytes to oxidative stress in the absence of the cellular prion protein. *Cell Mol Life Sci* 68(4): 687-96.
- Babula P, Masarik M, Adam V, Eckschlager T, Stiborova M, Trnkova L, Skutkova H, Provaznik I, Hubalek J, Kizek R. 2012. Mammalian metallothioneins: properties and functions. *Metallomics* 4(8): 739-50.
- Barberet P, Incerti S, Andersson F, Delalee F, Serani L, Moretto P. 2009. Technical description of the CENBG nanobeam line. *Nuclear Instruments & Methods in Physics Research Section B-Beam Interactions with Materials and Atoms* 267(12-13): 2003-2007.
- Beer C, Foldbjerg R, Hayashi Y, Sutherland DS, Autrup H. 2012. Toxicity of silver nanoparticles - nanoparticle or silver ion? *Toxicol Lett* 208(3): 286-92.
- Bell RA, Kramer JR. 1999. Structural chemistry and geochemistry of silver-sulfur compounds: Critical review. *Environmental Toxicology and Chemistry* 18(1): 9-22.

Brun E, Barreau F, Veronesi G, Fayard B, Sorieul S, Chaneac C, Carapito C, Rabilloud T, Mabondzo A, Herlin-Boime N, Carriere M. 2014. Titanium dioxide nanoparticle impact and translocation through ex vivo, in vivo and in vitro gut epithelia. *Part Fibre Toxicol* 11(13): 1743-8977.

Carmona A, Deves G, Ortega R. 2008. Quantitative micro-analysis of metal ions in subcellular compartments of cultured dopaminergic cells by combination of three ion beam techniques. *Anal Bioanal Chem* 390(6): 1585-94.

Carriere M, Gouget B, Gallien JP, Avoscan L, Gobin R, Verbavatz JM, Khodja H. 2005. Cellular distribution of uranium after acute exposure of renal epithelial cells: SEM, TEM and nuclear microscopy analysis. *Nuclear Instruments & Methods in Physics Research Section B-Beam Interactions with Materials and Atoms* 231: 268-273.

Chairuangkitti P, Lawanprasert S, Roytrakul S, Aueviriyavit S, Phummiratch D, Kulthong K, Chanvorachote P, Maniratanachote R. 2012. Silver nanoparticles induce toxicity in A549 cells via ROS-dependent and ROS-independent pathways. *Toxicol In Vitro* 27(1): 330-8.

Chernousova S, Epple M. 2013. Silver as antibacterial agent: ion, nanoparticle, and metal. *Angew Chem Int Ed Engl* 52(6): 1636-53.

Dineley KE, Votyakova TV, Reynolds IJ. 2003. Zinc inhibition of cellular energy production: implications for mitochondria and neurodegeneration. *J Neurochem* 85(3): 563-70.

Dos Santos CA, Seckler MM, Ingle AP, Gupta I, Galdiero S, Galdiero M, Gade A, Rai M. 2014. Silver nanoparticles: therapeutical uses, toxicity, and safety issues. *J Pharm Sci* 103(7): 1931-44.

Elechiguerra JL, Larios-Lopez L, Liu C, Garcia-Gutierrez D, Camacho-Bragado A, Yacamán MJ. 2005. Corrosion at the nanoscale: The case of silver nanowires and nanoparticles. *Chemistry of Materials* 17(24): 6042-6052.

Fabrega J, Fawcett SR, Renshaw JC, Lead JR. 2009. Silver Nanoparticle Impact on Bacterial Growth: Effect of pH, Concentration, and Organic Matter. *Environmental Science & Technology* 43(19): 7285-7290.

Gazaryan IG, Krasinskaya IP, Kristal BS, Brown AM. 2007. Zinc irreversibly damages major enzymes of energy production and antioxidant defense prior to mitochondrial permeability transition. *J Biol Chem* 282(33): 24373-80.

Hamilton JA. 1980. Macrophage stimulation and the inflammatory response to asbestos. *Environ Health Perspect* 34: 69-74.

Hedley DW, Chow S. 1994. Evaluation of methods for measuring cellular glutathione content using flow cytometry. *Cytometry* 15(4): 349-58.

Jiang X, Miclaus T, Wang L, Foldbjerg R, Sutherland DS, Autrup H, Chen C, Beer C. 2014. Fast intracellular dissolution and persistent cellular uptake of silver nanoparticles in CHO-K1 cells: implication for cytotoxicity. *Nanotoxicology*: 16.

Johnson LV, Walsh ML, Chen LB. 1980. Localization of mitochondria in living cells with rhodamine 123. *Proc Natl Acad Sci U S A* 77(2): 990-4.

Kaegi R, Voegelin A, Sinnet B, Zuleeg S, Hagendorfer H, Burkhardt M, Siegrist H. 2011. Behavior of Metallic Silver Nanoparticles in a Pilot Wastewater Treatment Plant. *Environmental Science & Technology* 45(9): 3902-3908.

Kim B, Park C-S, Murayama M, Hochella MF, Jr. 2010. Discovery and Characterization of Silver Sulfide Nanoparticles in Final Sewage Sludge Products. *Environmental Science & Technology* 44(19): 7509-7514.

Kim HR, Kim MJ, Lee SY, Oh SM, Chung KH. 2011. Genotoxic effects of silver nanoparticles stimulated by oxidative stress in human normal bronchial epithelial (BEAS-2B) cells. *Mutat Res* 726(2): 129-35.

Kittler S, Greulich C, Diendorf J, Koeller M, Epple M. 2010. Toxicity of silver nanoparticles increases during storage because of slow dissolution under release of silver ions. *Chemistry of Materials* 22(16): 4548-4554.

Lemire J, Mailloux R, Appanna VD. 2008. Zinc toxicity alters mitochondrial metabolism and leads to decreased ATP production in hepatocytes. *J Appl Toxicol* 28(2): 175-82.

Levard C, Hotze EM, Lowry GV, Brown GE, Jr. 2012. Environmental Transformations of Silver Nanoparticles: Impact on Stability and Toxicity. *Environmental Science & Technology* 46(13): 6900-6914.

Levard C, Reinsch BC, Michel FM, Oumahi C, Lowry GV, Brown GE, Jr. 2011. Sulfidation Processes of PVP-Coated Silver Nanoparticles in Aqueous Solution: Impact on Dissolution Rate. *Environmental Science & Technology* 45(12): 5260-5266.

Liu J, Pennell KG, Hurt RH. 2011. Kinetics and Mechanisms of Nanosilver Oxysulfidation. *Environmental Science & Technology* 45(17): 7345-7353.

Maxwell JA, Teesdale WJ, Campbell JL. 1995. THE GUELPH-PIXE SOFTWARE PACKAGE-II. *Nuclear Instruments & Methods in Physics Research Section B-Beam Interactions with Materials and Atoms* 95(3): 407-421.

Mayer M. 2002. Ion beam analysis of rough thin films. *Nuclear Instruments & Methods in Physics Research Section B-Beam Interactions with Materials and Atoms* 194(2): 177-186.

Meister A. 1988. Glutathione metabolism and its selective modification. *J Biol Chem* 263(33): 17205-8.

Mulley G, Jenkins AT, Waterfield NR. 2014. Inactivation of the antibacterial and cytotoxic properties of silver ions by biologically relevant compounds. *PLoS One* 9(4): 2014.

Navarro E, Piccapietra F, Wagner B, Marconi F, Kaegi R, Odzak N, Sigg L, Behra R. 2008. Toxicity of silver nanoparticles to *Chlamydomonas reinhardtii*. *Environ Sci Technol* 42(23): 8959-64.

Nishanth RP, Jyotsna RG, Schlager JJ, Hussain SM, Reddanna P. 2011. Inflammatory responses of RAW 264.7 macrophages upon exposure to nanoparticles: role of ROS-NFkappaB signaling pathway. *Nanotoxicology* 5(4): 502-16.

Oh N, Park JH. 2014. Endocytosis and exocytosis of nanoparticles in mammalian cells. *Int J Nanomedicine* 1: 51-63.

Park EJ, Yi J, Kim Y, Choi K, Park K. 2010. Silver nanoparticles induce cytotoxicity by a Trojan-horse type mechanism. *Toxicol In Vitro* 24(3): 872-8.

Pillai S, Behra R, Nestler H, Suter MJ, Sigg L, Schirmer K. 2014. Linking toxicity and adaptive responses across the transcriptome, proteome, and phenotype of *Chlamydomonas reinhardtii* exposed to silver. *Proc Natl Acad Sci U S A* 111(9): 3490-5.

Pratsinis A, Hervella P, Leroux JC, Pratsinis SE, Sotiriou GA. 2013. Toxicity of silver nanoparticles in macrophages. *Small* 9(15): 2576-84.

Ratte HT. 1999. Bioaccumulation and toxicity of silver compounds: A review. *Environmental Toxicology and Chemistry* 18(1): 89-108.

Reinsch BC, Levard C, Li Z, Ma R, Wise A, Gregory KB, Brown GE, Jr., Lowry GV. 2012. Sulfidation of Silver Nanoparticles Decreases *Escherichia coli* Growth Inhibition. *Environmental Science & Technology* 46(13): 6992-7000.

Sadauskas E, Danscher G, Stoltenberg M, Vogel U, Larsen A, Wallin H. 2009. Protracted elimination of gold nanoparticles from mouse liver. *Nanomedicine* 5(2): 162-9.

Schleicher U, Bogdan C. 2009. Generation, culture and flow-cytometric characterization of primary mouse macrophages. *Methods Mol Biol* 531: 203-24.

Setyawati MI, Yuan X, Xie J, Leong DT. 2014. The influence of lysosomal stability of silver nanomaterials on their toxicity to human cells. *Biomaterials* 35(25): 6707-15.

Singh RP, Ramarao P. 2012. Cellular uptake, intracellular trafficking and cytotoxicity of silver nanoparticles. *Toxicol Lett* 213(2): 249-59.

Sotiriou GA, Pratsinis SE. 2010. Antibacterial Activity of Nanosilver Ions and Particles. *Environmental Science & Technology* 44(14): 5649-5654.

Tian L, Lawrence DA. 1996. Metal-induced modulation of nitric oxide production in vitro by murine macrophages: lead, nickel, and cobalt utilize different mechanisms. *Toxicol Appl Pharmacol* 141(2): 540-7.

Triboulet S, Aude-Garcia C, Armand L, Collin-Faure V, Chevallet M, Diemer H, Gerdil A, Proamer F, Strub JM, Habert A, Herlin N, Van Dorsselaer A, Carriere M, Rabilloud T. 2015. Comparative proteomic analysis of the molecular responses of mouse macrophages to titanium dioxide and copper oxide nanoparticles unravels some toxic mechanisms for copper oxide nanoparticles in macrophages. *PLoS One* 10(4): 2015.

Triboulet S, Aude-Garcia C, Carriere M, Diemer H, Proamer F, Habert A, Chevallet M, Collin-Faure V, Strub JM, Hanau D, Van Dorsselaer A, Herlin-Boime N, Rabilloud T. 2013. Molecular responses of mouse macrophages to copper and copper oxide nanoparticles inferred from proteomic analyses. *Mol Cell Proteomics* 12(11): 3108-22.

Veronesi G, Aude-Garcia C, Kieffer I, Gallon T, Delangle P, Herlin-Boime N, Rabilloud T, Carriere M. 2015. Exposure-dependent Ag⁺ release from silver nanoparticles and its complexation in AgS₂ sites in primary murine macrophages *Nanoscale* 7(16): 7323-30.

Wang L, Zhang T, Li P, Huang W, Tang J, Wang P, Liu J, Yuan Q, Bai R, Li B, Zhang K, Zhao Y, Chen C. 2015. Use of Synchrotron Radiation-Analytical Techniques To Reveal Chemical Origin of Silver-Nanoparticle Cytotoxicity. *ACS Nano* 9(6): 6532-47.

Xiu Z-M, Ma J, Alvarez PJJ. 2011. Differential Effect of Common Ligands and Molecular Oxygen on Antimicrobial Activity of Silver Nanoparticles versus Silver Ions. *Environmental Science & Technology* 45(20): 9003-9008.

Xiu Z-m, Zhang Q-b, Puppala HL, Colvin VL, Alvarez PJJ. 2012. Negligible Particle-Specific Antibacterial Activity of Silver Nanoparticles. *Nano Letters* 12(8): 4271-4275.

Xu Y, Tang H, Liu JH, Wang H, Liu Y. 2013. Evaluation of the adjuvant effect of silver nanoparticles both in vitro and in vivo. *Toxicol Lett* 219(1): 42-8.

Yilma AN, Singh SR, Dixit S, Dennis VA. 2013. Anti-inflammatory effects of silver-polyvinyl pyrrolidone (Ag-PVP) nanoparticles in mouse macrophages infected with live *Chlamydia trachomatis*. *Int J Nanomedicine* 8: 2421-32.

Table 1. Silver fate, as determined by ICP-MS^a

Soluble fraction in fresh culture medium

Ag-NPs 24 h	1.5±0.2%
Ag-NPs 96 h	6.2±0.5%
Ag-lactate	19.5±2.9%

Soluble fraction in conditioned culture medium

Sc1A	7.0±0.1%
Sc1R	1.9±0.4%
Sc2	5.9±4.4%
Ag-lactate	16.2±0.4%

Uptake by cells

Sc1A	82.8±5.0%
Sc1R	41.0±12.0%
Sc2	64.4±1.7%
Ag-lactate	42.5±1.0%

Soluble fraction in cells

Sc1A	4.8±0.6%
Sc1R	4.6±0.9%†
Sc2	4.5±0.8%
Ag-lactate	47.8±1.9%†

^aResults are expressed as the percentage of the soluble Ag fraction (centrifuged supernatant) with respect to the total Ag content (uncentrifuged supernatant + pellet). Three independent experiments were carried out. †: p<0.01 compared to the acute condition.

Table 2. Summary of the results^a

	Sc1A	Sc1R	Sc2
Exposure condition	Acute	Acute and recovery	Repeated
Cell content	++	+	++
Cell distribution	Loose agglomerate and layered structure	Loose agglomerate and layered structure	Loose and dense agglomerates
Glutathione	-	+	=
Metallothionein	++	++	++
Mitochondria	-	-	-
Phagocytosis	--	-	-
NO production	--	-	=
PIC	++	=	+
AIC	--	-	-

^aAcute exposure, i.e. 24 h at 5 µg/mL Ag-NP; Acute and recovery exposure, i.e. 24 h at 5 µg/mL Ag-NP then 72 h in cell culture medium; repeated exposure, i.e. 4 days at 1.25 µg/mL. ++: high increase; +: low increase; --: high decrease; -: low decrease; =: no difference. "Cell content": measured by PIXE; "Cell distribution": observed by TEM, "Glutathione": intracellular glutathione content, "Metallothionein": metallothionein mRNA expression induction, "Phagocytosis": phagocytic activity of macrophages, "NO production": production of NO upon stimulation by LPS. "PIC": secretion of pro-inflammatory cytokines and "AIC": secretion of anti-inflammatory cytokines, measured after LPS stimulation.

Figure captions

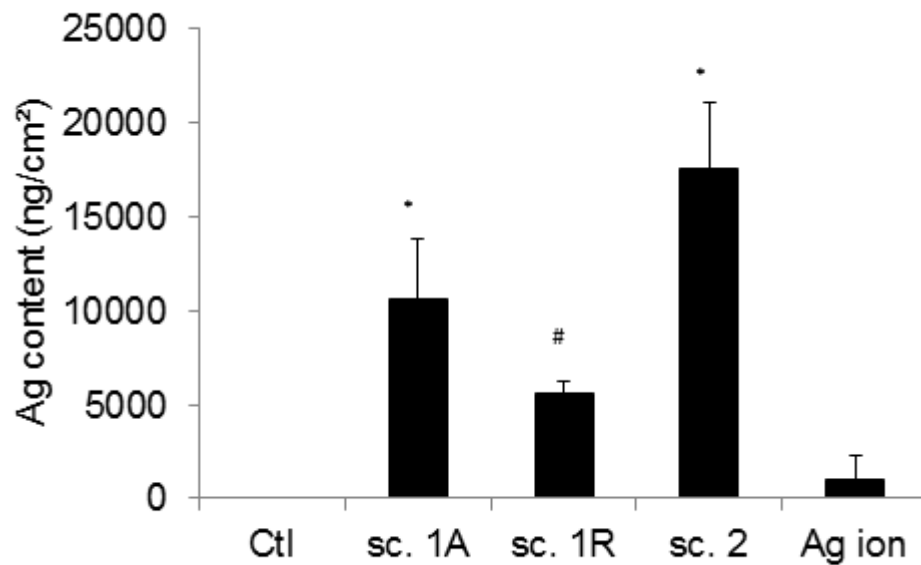


Figure 1. Intracellular Ag content. Ag content was quantified by particle-induced X-ray emission (PIXE) in unexposed cells, or macrophages exposed for 24 h to 5 $\mu\text{g}/\text{mL}$ Ag-NPs immediately after exposure (sc. 1A) or after 72 h of recovery in NP-free medium (sc. 1R), after repeated exposure to 1.25 $\mu\text{g}/\text{mL}$ Ag-NP per day for 4 days (sc. 2) or after 24 h of exposure to Ag lactate (5 μM). Bar graphs represent mean \pm standard deviation of 4 measurements. Student's T-test, * $p \leq 0.05$ vs. Ctl, # $p \leq 0.05$ vs. Ctl, sc. 1A and sc. 2.

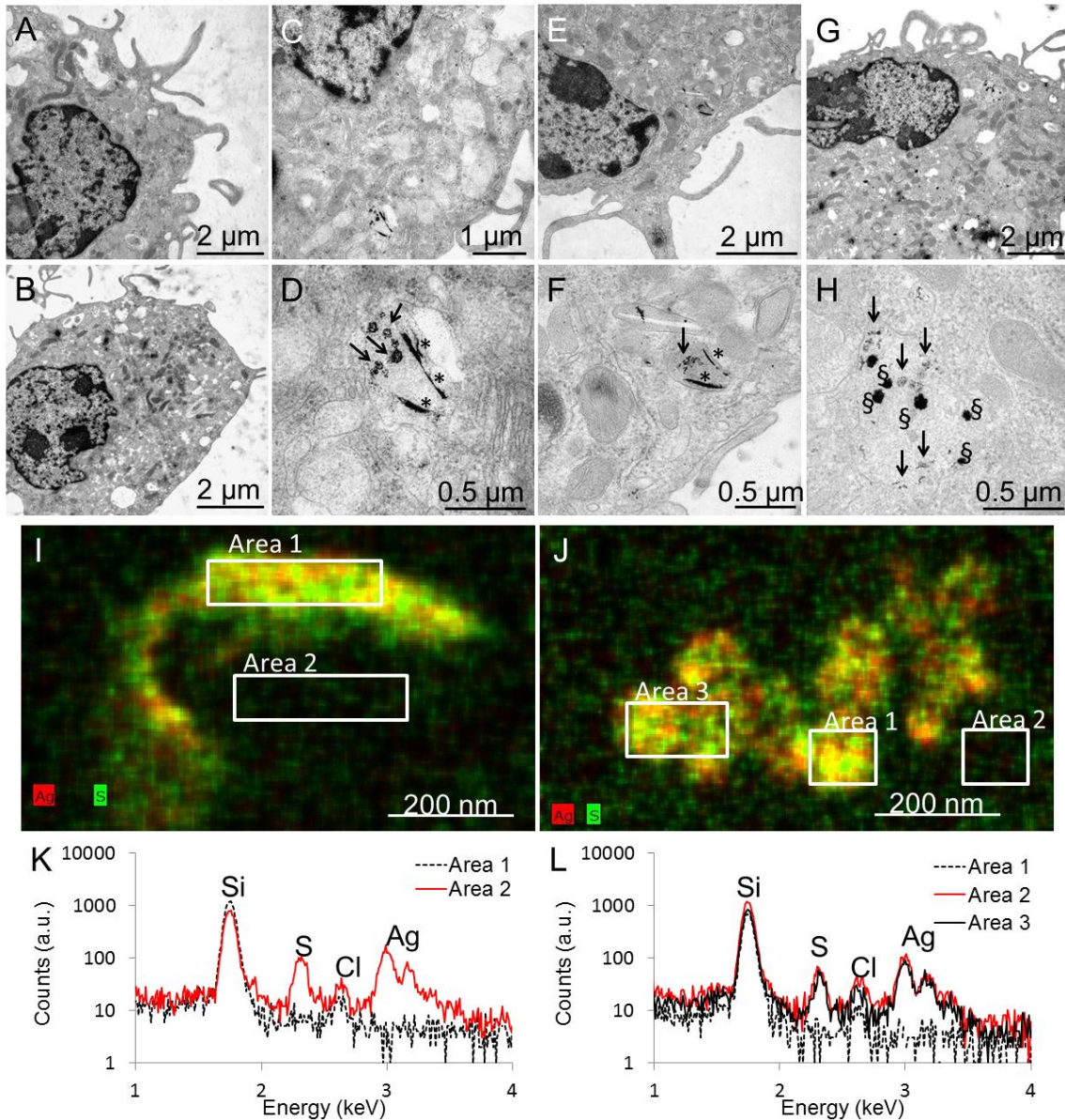


Figure 2. Scanning transmission electron microscopy (STEM) and energy dispersive spectroscopy (EDS) analyses of intracellular compartments containing electron-dense structures, in primary murine macrophages exposed to Ag-NPs. Unexposed cells (A-B) or cells exposed for 24 h to 5 μg/mL Ag-NPs (C-D) or cells exposed for 24 h to 5 μg/mL Ag-NPs and allowed to recover for 72 h in cell culture medium without NPs (E-F) or repeatedly exposed to 1.25 μg/mL Ag-NP per day for 4 days (G-H), then imbedded in epoxy resin, fixed with OsO₄, cut and observed in STEM. Ag distribution was then imaged by EDS in a layered structure observed

in cells exposed for 24 h to 5 $\mu\text{g}/\text{mL}$ Ag-NPs (I) or in a condensed structure observed in cells repeatedly exposed to 1.25 $\mu\text{g}/\text{mL}$ Ag-NP per day for 4 days (J). EDS spectra recorded in areas 1, 2 and 3 depicted in I and J are shown in K and L, respectively.

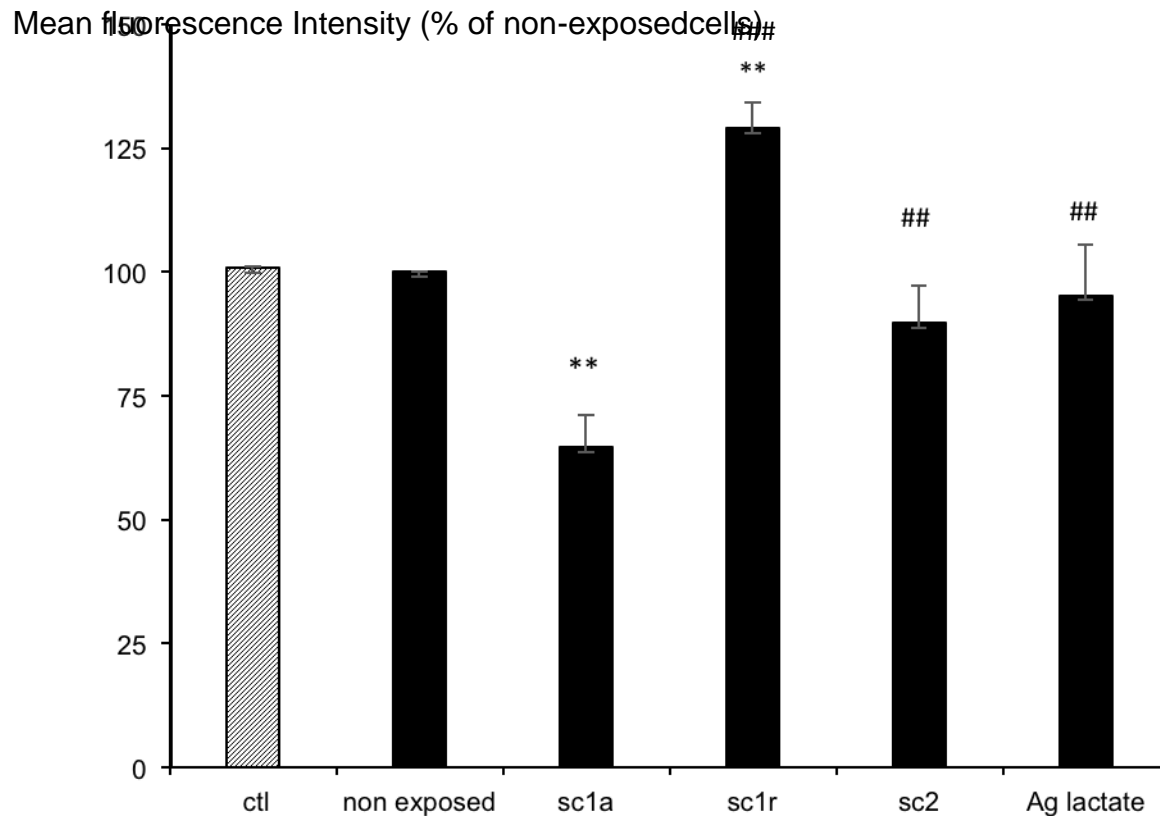


Figure 3. Quantification of GSH in Ag-NP-exposed cells. GSH content is expressed as the percentage of the fluorescence of monochlorobimane in exposed cells as compared to unexposed cells. "Control": cells exposed simultaneously to Ag-NPs and monochlorobimane. Measurements were carried out in triplicate on independent cultures. Statistical confidence (Student's T-test): ** $p \leq 0.01$ vs. control cells and ## $p \leq 0.01$, ### $p \leq 0.001$ vs. Sc1A.

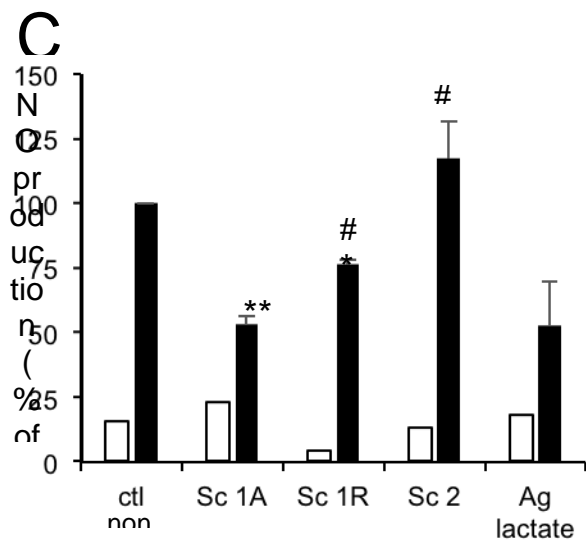
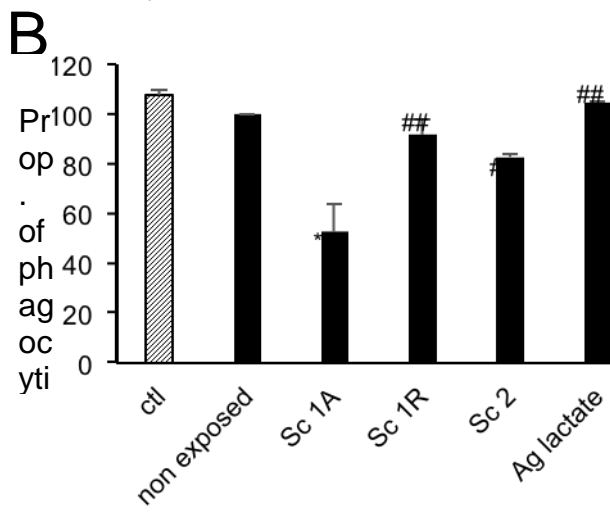
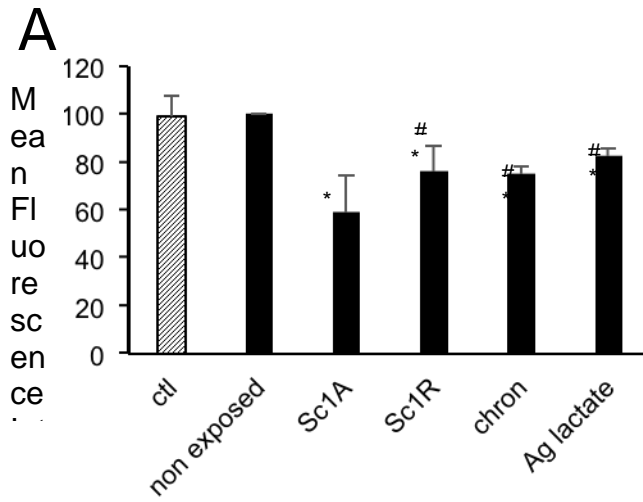


Figure 4. Consequences of an exposure to Ag-NPs on macrophage functionality. Mitochondrial transmembrane potential (A) assessed by measuring Rhodamine 123 internalization in cells. Results are expressed as the percentage of fluorescence in Ag-NP-exposed cells vs. in unexposed cells. "Control": Ag-NPs were added to cells simultaneously to Rhodamine 123. Macrophages phagocytic capacity (B) measured in cells exposed to Ag-NPs, then to fluorescent beads, followed by cell fluorescence quantification by flow cytometry. Results are expressed as the percentage of phagocytic activity in Ag-NP-exposed cells with respect to non-exposed cells. "Control": Ag-NPs were added to cells simultaneously to latex beads. Nitric oxide production (C) in macrophages that were not stimulated (white bars) or stimulated by LPS (black bars). Measurements were carried out at least 3 times. Statistical confidence (Student's T-test): * $p \leq 0.05$, ** $p \leq 0.01$, *** $p \leq 0.001$ vs. control cells and # $p \leq 0.05$, ## $p \leq 0.01$ vs Sc1A.

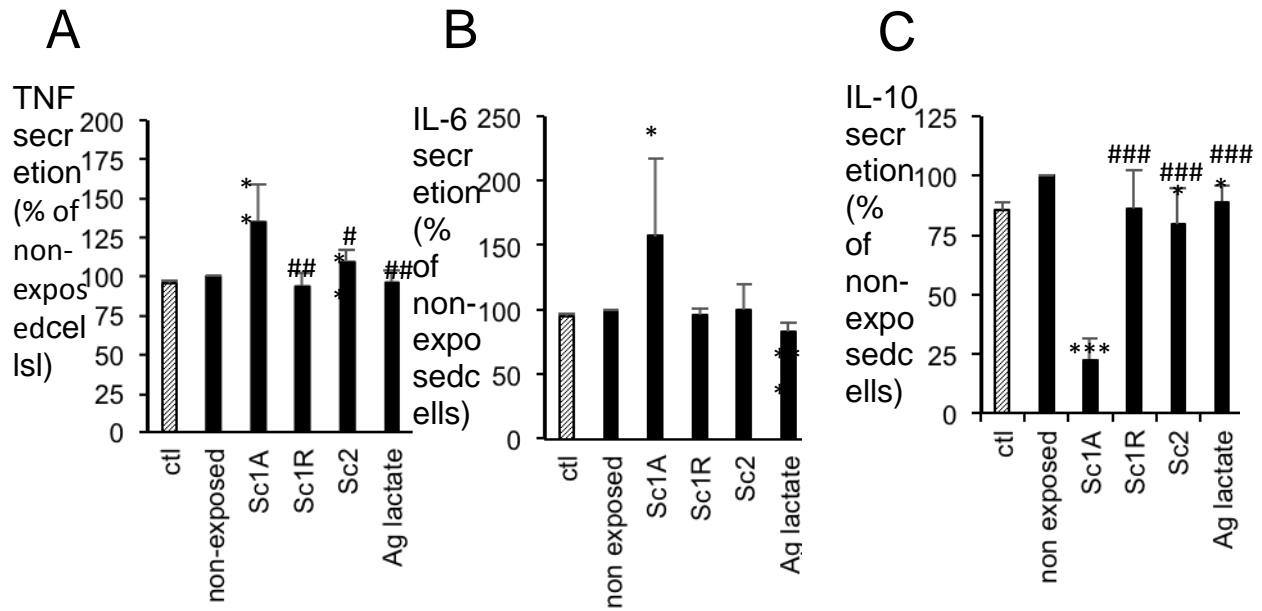


Figure 5. Impact of Ag-NPs on cytokine production by macrophages. $\text{TNF}\alpha$ (A), IL-6 (B) and IL-10 (C) secretion by the macrophages exposed to Ag-NPs or Ag-lactate then stimulated by LPS, assessed using CBA assay and flow cytometry measurement. Results are expressed as the percentage of secretion in exposed cells as compared to unexposed cells. "Control": unexposed cells to which Ag-NPs were added just before performing the CBA assay. Measurements were carried out at least 3 times. Statistical confidence (Student's T-test): * $p \leq 0.05$, ** $p \leq 0.01$, *** $p \leq 0.001$ vs. control cells and # $p \leq 0.05$, ## $p \leq 0.01$, ### $p \leq 0.001$ vs Sc1A.